

ANALYSIS OF CONVERGENCE ACCELERATION TECHNIQUES USED IN UNSTRUCTURED ALGORITHMS IN THE SOLUTION OF AERONAUTICAL PROBLEMS - PART I

Edisson Sávio de Góes Maciel

Rua Demócrito Cavalcanti, 152 - Afogados
Recife – PE – Brazil - CEP 50750-080
e-mail: edissonsavio@yahoo.com.br

Abstract. *This work intends to study convergence accelerating techniques applied to the solution of steady state problems. Techniques like spatially variable time step, implicit residual smoothing, enthalpy damping and increase of the CFL number during iterative process are studied. The Jameson and Mavriplis explicit algorithm, with centered spatial discretization and the artificial dissipation operator of Mavriplis, was implemented to perform the two-dimensional numerical experiments. This scheme is second order accurate in space. The Euler equations in conservative form, employing a finite volume formulation and an unstructured spatial discretization are solved. The techniques were studied and compared with themselves in the solution of the physical problem of the transonic flow around a NACA 0012 airfoil, with zero angle of attack. The employed time march algorithm was the Runge-Kutta method of five stages and second order. The results have shown that the best technique studied was enthalpy damping, having better convergence gain than the others and have moderate computational cost. A final analysis of the technique computational performances is accomplished at the end (cost, maximum CFL number and iterations to convergence).*

Keywords: *Spatially variable time step, Implicit residual smoothing, Enthalpy damping, Increase of CFL, Unstructured algorithm.*

1. Introduction

A point of intense research in CFD, Computational Fluid Dynamics, is the development of convergence acceleration techniques to steady state problems. The great amount of aerodynamics data required for aeronautical and aerospace vehicle design are obtained from these problems: Kutler (1985); Stiles and Hoffman (1985); and Nicola, Tognaccini, Visingardi and Paparone (1994); and others. Convergence acceleration techniques always were great objectives of CFD following the development of fluid mechanics equation solvers. A great amount of techniques were elaborated and several works tried to develop convergence acceleration computational tools which produce more efficient and, at the same time, less expensive codes.

On the context of convergence gains, an efficient technique that raised to numerical calculation was the “multigrid” procedure. Such technique was initially presented to obtain solutions of problems involving elliptic partial differential equations (Brandt, 1981) and, posteriorly, was extended to hyperbolic partial differential equations. Some works that used this procedure were: Jameson and Mavriplis (1986); Mavriplis (1988); Radespiel (1989); and Mavriplis (1995).

Techniques of convergence acceleration simpler and less expensive to explicit and implicit schemes, when applied to the solution of fluid mechanics equations, also were studied: spatially variable time step, enthalpy damping, residual smoothing and increase of CFL number during the iterative process. The spatially variable time step aims to use the maximum time step allowed by a local stability limit in each computational cell. This technique was initially applied by Jameson, Schmidt and Turkel (1981). Other works that used such technique were: Jameson and Mavriplis (1986); Mavriplis (1990); Swanson and Radespiel (1991); Luo, Baum and Löhner (1994); and Radespiel and Swanson (1995).

The enthalpy damping strategy is based on the fact that the Euler equations are inviscid and the total enthalpy keeps constant in all computational domain when the steady state is reached and the mass and the energy equations are satisfied. Forcing terms proportional to the difference between local total enthalpy and the freestream total enthalpy are added to the mass, momentum and energy conservation equations, aiming to accelerate the convergence process to steady state condition. This procedure was suggested by Jameson, Schmidt and Turkel (1981). Others works were: Jameson and Mavriplis (1986); Baruzzi, Habashi and Hafez (1991) and Long, Khan and Sharp (1991).

The maximum time step that can be used is limited by the CFL condition (Courant, Friedrichs and Lewy, 1928), which defines that the dependence domain of the discretized equations need no minimal contains the dependence domain of the original differential equation. To reduce this restriction, an implicit residual smoothing is developed to increase the scheme stability. Such strategy consists in determining an average residual value, weighted by neighbor residual values. This technique was introduced by Jameson and Mavriplis (1986) work. Others works were: Mavriplis (1990); Long, Khan and Sharp (1991); Luo, Baum and Löhner (1994); and Radespiel and Swanson (1995).

Other convergence acceleration technique simpler than the others is the increase of the CFL number during the convergence process to reach steady state. This technique consists in increasing the CFL number all time that a prescribed number of iterations is reached. The user determines the number of iterations to increase the CFL as the increase value to be considered too.

This work presents some convergence acceleration techniques generally applied to CFD community. The objective of this article is to present the best results obtained, in terms of convergence ratio and computational cost, for the studied techniques. The spatially variable time step, the implicit residual smoothing, the enthalpy damping and the

increase of the CFL number are the techniques studied. The Jameson and Mavriplis (1986) scheme, on an unstructured context, is used to generate the numerical results to comparison. Tests with a NACA 0012 airfoil configuration, involving transonic flow, were performed. The results have indicated that the enthalpy damping is the best choice among the techniques studied.

An unstructured discretization of the spatial domain is often recommended to complex configurations due to the facility and efficiency of domain discretization (Jameson and Mavriplis, 1986, and Mavriplis, 1990). However, the unstructured generation question will not be studied in this work.

2. Euler equations

The fluid movement is governed by the Euler equations, which express the mass, momentum and energy conservations of an inviscid, heat non-conductor and compressible mean, in the absence of external forces. In integral and conservative forms, these equations can be represented by:

$$\frac{\partial}{\partial t} \int_V Q dV + \int_S (E_e n_x + F_e n_y) dS = 0, \quad (1)$$

where Q is written to a Cartesian system, V is the volume of a cell, n_x and n_y are normal unity vectors in relation to each flux face, S is the flux area and E_e and F_e represent the convective flux vector components. Q , E_e and F_e are represented by:

$$Q = \begin{Bmatrix} \rho \\ \rho u \\ \rho v \\ e \end{Bmatrix}, \quad E_e = \begin{Bmatrix} \rho u \\ \rho u^2 + p \\ \rho uv \\ (e + p)u \end{Bmatrix} \quad \text{and} \quad F_e = \begin{Bmatrix} \rho v \\ \rho uv \\ \rho v^2 + p \\ (e + p)v \end{Bmatrix}, \quad (2)$$

where ρ is the fluid density; u and v are Cartesian components of the velocity vector in the x and y directions, respectively; e is the total energy per unity volume; and p is the static pressure. Expressions to the flux area S and to the volumes V are available in Maciel and Azevedo (2001) and in Maciel (2002).

The nondimensionalization applied to the Euler equations for all problems was accomplished in relation to the freestream density, ρ_∞ , and freestream speed of sound, a_∞ . Hence, the density is nondimensionalized in relation to ρ_∞ , the velocity components u and v are nondimensionalized in relation to a_∞ and the pressure and the total energy are nondimensionalized in relation to the product $\rho_\infty (a_\infty)^2$. The matrix system of the Euler equations is closed using the perfect gas state equation $p = (\gamma - 1) \left[e - 0.5 \rho (u^2 + v^2) \right]$ with γ being the ratio of specific heats. The total enthalpy is determined by $h = [\gamma / (\gamma - 1)] (p / \rho) + 0.5 (u^2 + v^2)$.

3. Jameson and Mavriplis (1986) algorithm

The Euler equations in conservative and integral forms, according to a finite volume formulation, can be written, on a context of unstructured spatial discretization (Jameson, Schmidt and Turkel, 1981, Jameson and Mavriplis, 1986, Maciel and Azevedo, 2001, and Maciel, 2002), as:

$$d(V_i Q_i) / dt + C(Q_i) = 0, \quad (3)$$

where $C(Q_i) = \sum_{k=1}^3 [E_e(Q_{i,k}) \Delta y_{i,k} - F_e(Q_{i,k}) \Delta x_{i,k}]$ is the discrete approximation to the flux integral of Eq. (1). In this work, it was adopted that:

$$Q_{i,k} = 0.5(Q_i + Q_k), \quad \Delta y_{i,k} = y_{n2} - y_{n1} \quad \text{and} \quad \Delta x_{i,k} = x_{n2} - x_{n1}, \quad (4)$$

with “ i ” indicating a given mesh volume and “ k ” being its respective neighbor; and $n1$ and $n2$ represent consecutive nodes of volume “ i ”, in counter-clockwise orientation.

The spatial discretization proposed by the authors is equivalent to a centered scheme with second order of accuracy, on a finite difference context. The introduction of a dissipation operator “ D ” is necessary to guarantee numerical stability in the presence, for example, of even-odd uncoupled solutions and nonlinear instabilities, like shock waves. So, Equation (3) is rewritten as:

$$d(V_i Q_i) / dt + [C(Q_i) - D(Q_i)] = 0. \quad (5)$$

The time integration is accomplished using a Runge-Kutta explicit method of second order and five stages and can be represented in generalized form as:

$$\begin{aligned} Q_i^{(0)} &= Q_i^{(n)} \\ Q_i^{(k)} &= Q_i^{(0)} - \alpha_k \Delta t_i / V_i \left[C(Q_i^{(k-1)}) - D(Q_i^{(m)}) \right], \\ Q_i^{(n+1)} &= Q_i^{(k)} \end{aligned} \quad (6)$$

where $k = 1, \dots, 5$; $m = 0$ to 4 ; $\alpha_1 = 1/4$, $\alpha_2 = 1/6$, $\alpha_3 = 3/8$, $\alpha_4 = 1/2$ e $\alpha_5 = 1$. The artificial dissipation operator should be evaluated only in the first two stages ($m = 0$, $k = 1$, e $m = 1$, $k = 2$), aiming CPU time economy, according to Swanson and Radespiel (1991). It is freezed for the reminiscent stages, exploring the hyperbolic properties of the Euler equations, aiming to guarantee steady state condition.

3.1. Artificial dissipation operator

The artificial dissipation operator employed in this work is based on Mavriplis (1990) and can be described as:

$$D(Q_i) = d^{(2)}(Q_i) - d^{(4)}(Q_i), \quad (7)$$

where: $d^{(2)}(Q_i) = \sum_{k=1}^3 0,5 \varepsilon_{i,k}^{(2)} (A_i + A_k) (Q_k - Q_i)$, named undivided Laplacian operator, is responsible to the numerical stability in the presence of shock waves; and $d^{(4)}(Q_i) = \sum_{k=1}^3 0,5 \varepsilon_{i,k}^{(4)} (A_i + A_k) (\nabla^2 Q_k - \nabla^2 Q_i)$, named biharmonic operator, is responsible to the background stability (for example, even-odd instabilities). In this last term, $\nabla^2 Q_i = \sum_{k=1}^3 (Q_k - Q_i)$.

Every time that “ k ” represents a special boundary cell, named “ghost” cell, its contribution in terms of $\nabla^2 Q_k$ is extrapolated from its real neighbor volume. The ε terms are defined as:

$$\varepsilon_{i,k}^{(2)} = K^{(2)} \text{MAX} (v_i, v_k) \quad \text{and} \quad \varepsilon_{i,k}^{(4)} = \text{MAX} \left[0, \left(K^{(4)} - \varepsilon_{i,k}^{(2)} \right) \right], \quad (8)$$

where $v_i = \sum_{k=1}^3 |p_k - p_i| / \sum_{k=1}^3 (p_k + p_i)$ represents a pressure sensor. It is employed to identify regions of high gradients. $K^{(2)}$ and $K^{(4)}$ are constants and typical values are $1/4$ and $3/256$, respectively. Every time that “ k ” represents a ghost cell, $v_g = v_i$. The A_i terms are contributions of the maximum normal eigenvalue of the Euler equations integrated along each cell face. They are defined as:

$$A_i = \sum_{k=1}^3 \left[|u_{i,k} \Delta y_{i,k} - v_{i,k} \Delta x_{i,k}| + a_{i,k} \left(\Delta x_{i,k}^2 + \Delta y_{i,k}^2 \right)^{0,5} \right], \quad (9)$$

where $u_{i,k}$, $v_{i,k}$ and $a_{i,k}$ are calculated by arithmetical average between values of properties associated with volume “ i ” and its respective neighbor “ k ”.

4. Convergence acceleration techniques

4.1. Spatially variable time step

The basic idea of this procedure consists in keeping a constant CFL number in all calculation domain, allowing that appropriated time steps to each specific mesh region could be used during the convergence process. Hence, and according to the CFL number definition, it is possible to write:

$$\Delta t_{cell} = CFL(\Delta s)_{cell} / c_{cell}, \quad (10)$$

where CFL is the “Courant-Friedrichs-Lewy” number to provide numerical stability to the scheme;

$c_{cell} = \left[(u^2 + v^2)^{0.5} + a \right]_{cell}$ is the maximum characteristic velocity of information propagation in the calculation domain; and $(\Delta s)_{cell}$ is a characteristic length of information propagation. On a finite volume context, $(\Delta s)_{cell}$ is chosen as the minimum value found between the centroid distance, involving cell “ i ” and its neighbor “ k ”, and the minimum cell side length.

4.2. Implicit residual smoothing

The implicit residual smoothing technique employed in this work is based on Jameson and Mavriplis (1986) article. The residual is initially defined as follows:

$$R(Q) = I/V [C(Q) - D(Q)]. \quad (11)$$

The smoothing is performed replacing the residual associated with a given computational cell by the average residual \bar{R} , obtained by the solution of the equation:

$$\bar{R} - \varepsilon \nabla^2 \bar{R} = R, \quad (12)$$

where to a cell centered data base,

$$\nabla^2 \bar{R} = \sum_{k=1}^{tnnc} (\bar{R}_k - \bar{R}), \quad (13)$$

with “ k ” being the index of the neighbor cell of the respective cell under study and “ $tnnc$ ” is the total number of neighbor cells. The Equation (12) represents a diagonal dominant system and due to its high cost to solution, Jameson and Mavriplis (1986) suggest that a few iterations with the Jacobi method are sufficient to obtain residual smoothing. The resultant algorithm to the solution of Eq. (12) is written as:

$$(I + tnnc \times \varepsilon) \bar{R}^{(m)} = R + \varepsilon \sum_{k=1}^{tnnc} \bar{R}_k^{(m-1)}, \quad (14)$$

where $\bar{R}^{(0)} = R$. Jameson and Mavriplis (1986) suggest that only two iterations are necessary to solve Eq. (14), to steady state problems. These authors also suggest that the implicit residual smoothing should be accomplished in alternate stages of the time integration method with the purpose of computational cost reduction. The parameter ε assumes values between 0.0 and 1.0, 0.5 is the value suggested by Jameson and Mavriplis (1986).

4.3. Enthalpy damping

The enthalpy damping technique suggested by Jameson, Schmidt and Turkel (1981) article is applied to the Euler equations in this work to accelerate the convergence process to steady state. In this technique, forcing terms proportional to the difference between the local total enthalpy and the freestream total enthalpy are added to each conservation equation.

The conservation equation system is written as:

$$\partial/\partial t \int_V Q dV + \int_S (E_e n_x + F_e n_y) dS - \int_V Z dV = 0, \quad (15)$$

where $Z = -(H - H_\infty) \beta [\rho \quad \rho u \quad \rho v \quad \rho H]^T$ and β is an user specified coefficient. The forcing terms do not alter the steady state solution if the physical problem satisfies the constant total enthalpy condition.

In centered schemes, the artificial dissipation operator often introduces variations in the total enthalpy, which produces a non-conservative effect to this property. Mavriplis (1988) suggests that the artificial dissipation provided by the operator in the energy equation should be imposed to the total enthalpy “ ρH ” as conserved variable. It guarantees the constant total enthalpy in the field and allows the application of the enthalpy damping technique.

4.4. Increase of the CFL number

This procedure consists in increase the CFL number during the convergence process every time that a determined number of iterations is performed by the solver. The user specifies the number of iterations to increase the CFL number

and its increase value too.

5. Initial and boundary conditions

5.1. Initial condition

Values of freestream flow are adopted to all properties as initial condition for this problem, in all computational domain (Jameson and Mavriplis, 1986). Therefore, the vector of conserved variables is defined as:

$$Q_i = \left\{ 1 \quad M_\infty \cos \alpha \quad M_\infty \sin \alpha \quad \frac{1}{\gamma(\gamma-1)} + 0.5M_\infty^2 \right\}^T, \quad (16)$$

where M_∞ is the freestream Mach number and α is the attack angle.

5.2. Boundary conditions

The boundary conditions are basically of four types: solid wall, entrance, exit and continuity. These conditions are implemented, as commented before, in ghost cells.

(a) Wall condition: This condition imposes the flow tangency at solid wall. This condition is satisfied considering the tangent velocity component of the ghost volume at wall as equal to the respective velocity component of its real neighbor cell. At the same way, the normal velocity component of the ghost volume at wall is equal in value, but with opposite signal, to the respective velocity component of its real neighbor cell.

The normal pressure gradient of the fluid to the wall is assumed be equal to zero according to an inviscid formulation. The same hypothesis is applied to the normal temperature gradient to the wall. From these considerations, the density and pressure of the ghost volume are extrapolated from the respective values of its real neighbor volume (zero order extrapolation). The total energy is obtained by the state equation of a perfect gas.

(b) Entrance condition:

(b.1) Subsonic flow: Three properties are specified and one extrapolated, based on information propagation analysis along characteristic directions in the calculation domain (Maciel and Azevedo, 1997, and Maciel and Azevedo, 1998). In other words, to subsonic flow, three characteristic directions of propagation information point inward to the computational domain and should be fixed. Just the characteristic direction associated to the “ (q_n-a) ” velocity can not be specified and should be determined by interior information from the calculation domain. The pressure was the extrapolated variable from the real neighbor volumes, for the problem studied. Density and velocity components adopted values of freestream flow. The total energy is determined by the state equation of a perfect gas.

(b.2) Supersonic flow: All variables are fixed with values of freestream flow.

(c) Exit condition:

(c.1) Subsonic flow: Three characteristic directions of propagation information point outward to the computational domain. Hence, the associated variables should be extrapolated from interior information. The characteristic direction associated to the “ (q_n-a) ” velocity should be specified because it point inward to the computational domain. In this case, the ghost volume pressure is specified from its initial value. Density and velocity components are extrapolated and total energy is obtained from the state equation of a perfect gas.

(c.2) Supersonic flow: All variables are extrapolated from interior domain due to all four characteristic directions of information propagation of the Euler equations point outward to the computational domain and, therefore, nothing can be fixed.

(d) Continuity condition: It is necessary that the flow continuity at the trailing edge should be satisfied (Kutta condition). This condition is assured to impose that the conserved variable vector at lower body surface should be equal to the conserved variable vector at upper body surface.

6. Results

Tests were performed in a CELERON-1.2GHz and 128 Mbytes of RAM memory microcomputer. Converged results occurred to 4 orders of reduction of the maximum residual value. The parameter γ assumed a value of 1.4. A zero attack angle was adopted to the airfoil problem.

6.1. Airfoil physical problem

A mesh of type “O” of 49x100 points or composed of 9,504 triangular volumes and 4,900 nodes around the airfoil was used. An exponential stretching of 5% was used in the normal direction to the airfoil surface. The far field boundary (entrance and exit boundaries) was located at 10.0 chords in relation to airfoil’s leading edge. The mesh is

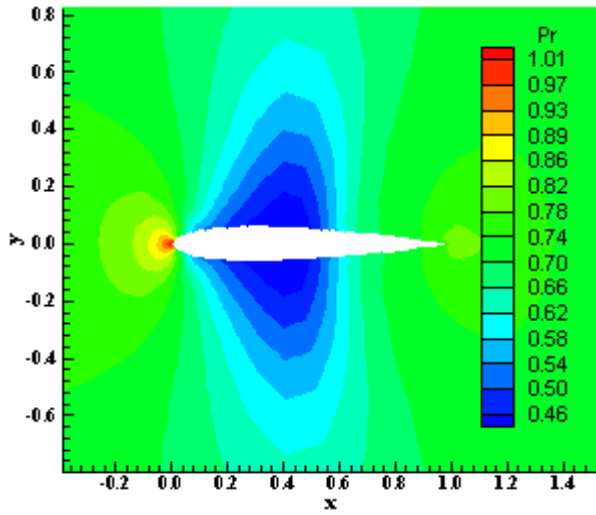


Figure 1. Pressure field.

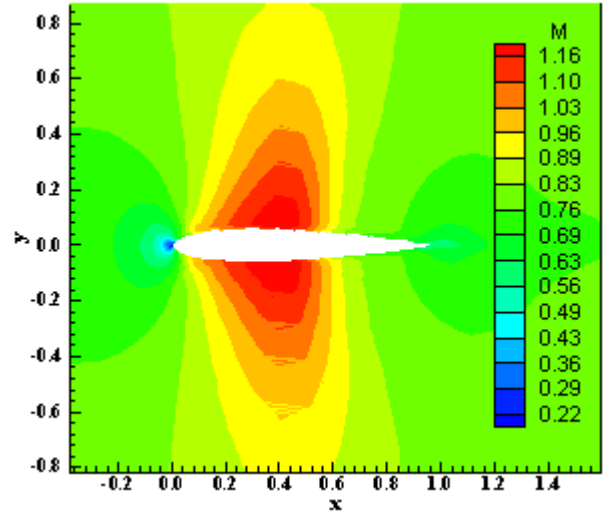


Figure 2. Mach number field.

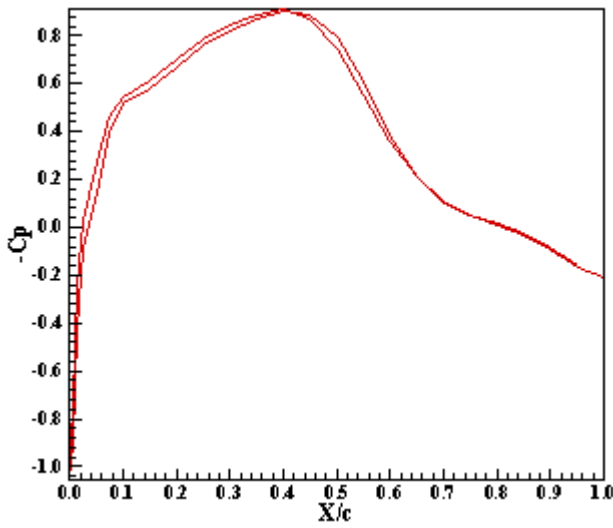


Figure 3. $-C_p$ distribution.

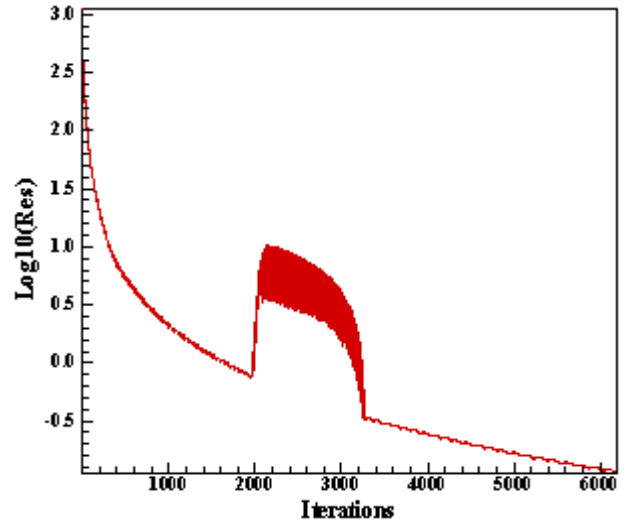


Figure 4. Convergence history.

structured but the spatial discretization of the Euler equations is unstructured. All indexing tables are generated to the algorithm execution.

The freestream Mach number adopted to the numerical simulation was 0.8, characterizing a transonic flow regime. A CFL number of 0.7 was used by the Jameson and Mavriplis (1986) scheme, using a constant time step. The convergence was obtained in 6,199 iterations.

Figures 1 and 2 show the pressure and Mach number contours, while Fig. 3 and Fig. 4 show the $-C_p$ distribution around the airfoil and the convergence history, respectively. The computational cost of the Jameson and Mavriplis (1986) algorithm using a constant time step is 0.0000186s/per volume/per iteration.

6.2. Spatially variable time step

The spatially variable time step accelerated the convergence process of the Jameson and Mavriplis (1986) scheme. A CFL number of 0.5, less than that used to the constant time step case, was used and the convergence occurred in 4,920 iterations, with a computational cost of 0.0000558s/per volume/per iteration. The CFL number equals to 0.5 was the maximum value allowed using the spatially variable time step technique. This cost is about 200% more expensive than that obtained with the constant time step case, without convergence acceleration technique. The gain in terms of iterations to convergence is of 20.6%. So, the computational cost is more expensive but there is a meaningful convergence gain.

6.3. Implicit residual smoothing

To use this technique the time step was kept constant and the residual smoothing was accomplished in odd stages of the time integration method.

The CFL number used was 0.7, kept constant during the numerical experiments. Table 1 shows the values of ε used and the number of convergence iterations. The best result occurred to $\varepsilon = 0.18$, presenting convergence in 4,686 iterations.

Table 1. Values of ε and the respective iterations to convergence.

Value of ε :	Iterations to convergence:	Value of ε :	Iterations to convergence:
0.10	5,218	0.17	4,774
0.15	4,874	0.18	4,686

The computational cost of this technique was 0,0000581s/per volume/per iteration, which corresponds to about 212.4% more expensive than that used with a constant time step. The computational gain, taking into account the best performance, was 24.4%, which is better than that obtained with the spatially variable time step. The CPU time of this technique is higher than that of the spatially variable time step, which is a limiting factor too.

6.4. Enthalpy damping

The time step was kept constant during the simulations and a CFL number of 0.7 was used. Table 2 shows values of β with the respective number of iterations to reach the steady state condition. Values of β were adopted between 0.1 and 1.0. The maximum value of 1.0 to this parameter was determined aiming do not meaningfully alter the pressure and the Mach number fields. Although greater values of β can be used, meaningful modifications occur in the pressure and Mach number contours that alter the solution.

Table 2. Values of β and the respective iterations to convergence.

Value of β :	Iterations to convergence:	Value of β :	Iterations to convergence:
0.10	5,882	0.60	4,768
0.20	5,587	0.70	4,549
0.30	5,311	0.80	4,429
0.40	5,157	0.90	4,307
0.50	4,914	1.00	4,195

The computational cost of this technique is 0.0000431s/per volume/per iteration, which is about 131.7% more expensive than that of the constant time step. The computational gain in terms of convergence acceleration was 32.3%, in relation to the best convergence, better than the first two initial techniques. A limiting factor is that this technique can only be applied to the Euler equations, which is the case where the total enthalpy keeps constant in all computational domain.

6.5. Increase of CFL

The last technique studied did not present converged results; or better, the idea of increase the CFL number in 500 iterations, 1,000 iterations, 2,000 iterations and even 3,000 iterations resulted in divergent results. This fact limits the use of this technique to problems in which the convergence is easier. The airfoil case is more severe than other classical problems because there is a shock wave formed in about 40% of the leading edge and the flow regime is transonic, which leads to a higher difficult to the algorithm in treat propagation of information in the calculation domain.

7. Conclusions

In this work was presented four techniques of convergence acceleration implemented in the Jameson and Mavriplis (1986) scheme, on the context of unstructured discretization of the Euler equations. A constant time step solution, without any acceleration technique, was initially presented. Posteriorly, the techniques of implicit residual smoothing and enthalpy damping were always applied considering a constant time step aiming to compare with initial results. The physical problem of the transonic flow around a NACA 0012 airfoil was studied. This problem presents a major difficult in terms of convergence in relation to other classical problems because there is a shock wave formed over and under the airfoil and there is the transition between subsonic and supersonic flow.

The numerical experiments have shown that the enthalpy damping technique presents better relation cost-benefit among the techniques studied. Unfortunately, the increase of CFL technique proportioned divergent results, avoiding the analysis of its potential. At the same time, the increase of CFL technique demonstrates its higher limitation than the others techniques to treat more complex physical problems.

The computational gain of 32.3% of the enthalpy damping is meaningful even due to the increase of CPU time in relation to the constant time step case. The implicit residual smoothing was in second place, with a computational gain

of 24.4% and in third place was the spatially variable time step procedure, with a computational gain of 20.6%. All three techniques which present converged solutions have a certain empirical degree represented by the choice of the initial CFL number or the choice of values to the parameters ε or β . The user chooses the parameter which prefers. The enthalpy damping technique has the limitation of only be applied to the potential or the Euler equations.

8. Acknowledgements

The author thanks the financial support conceded by CNPq under the form of scholarship of process number 304318/2003-5, DCR/1F.

9. References

- Baruzzi, G. S., Habashi, W. G. and Hafez, M. M., 1991, "Finite Element Solutions of the Euler Equations for Transonic External Flows", *AIAA Journal*, Vol. 29, No. 11, pp. 1886-1893.
- Brandt, A., 1981, "Guide to Multigrid Development", *Lecture Notes in Mathematics*, Vol. 960, Springer-Verlag, Berlin, pp. 220-312.
- Courant, R., Friedrichs, K. O., and Lewy, H., 1928, "Ueber Die Differenzengleichungen Der Mathematischen Physik", *Mathematical Annual*, Vol. 100, p. 32.
- Jameson, A. and Mavriplis, D., 1986, "Finite Volume Solution of the Two-Dimensional Euler Equations on a Regular Triangular Mesh", *AIAA Journal*, Vol. 24, No. 4, pp. 611-618.
- Jameson, A., Schmidt, W. and Turkel, E., 1981, "Numerical Solution of the Euler Equations by Finite Volume Methods Using Runge-Kutta Time Stepping Schemes", *AIAA Paper* 81-1259.
- Kutler, P., 1985, "A Perspective of Theoretical and Applied Computational Fluid Dynamics", *AIAA Journal*, Vol. 23, No. 3, pp. 328-341.
- Long, L. N., Khan, M. N. S. and Sharp, H. T., 1991, "Massively Parallel Three-Dimensional Euler / Navier-Stokes Method", *AIAA Journal*, Vol. 29, No. 5, pp. 657-666.
- Luo, H., Baum, J. D. and Löhner, R., 1994, "Edge-Based Finite Element Scheme for the Euler Equations", *AIAA Journal*, Vol. 32, No. 6, pp. 1183-1190.
- Maciel, E. S. G. and Azevedo, J. L. F., 1997, "Comparação entre Vários Algoritmos de Fatoração Aproximada na Solução das Equações de Navier-Stokes", *Proceedings of the 14th Brazilian Congress of Mechanical Engineering* (available in CD-ROM), Bauru, SP, Brazil.
- Maciel, E. S. G. and Azevedo, J. L. F., 1998, "Comparação entre Vários Esquemas Implícitos de Fatoração Aproximada na Solução das Equações de Navier-Stokes", *RBCM- Journal of the Brazilian Society of Mechanical Sciences*, Vol. XX, No. 3, pp. 353-380.
- Maciel, E. S. G. and Azevedo, J. L. F., 2001, "Solution of Aerospace Problems Using Structured and Unstructured Strategies", *RBCM- Journal of the Brazilian Society of Mechanical Sciences*, Vol. XXIII, No. 2, pp. 155-178.
- Maciel, E. S. G., 2002, "Simulação Numérica de Escoamentos Supersônicos e Hipersônicos Utilizando Técnicas de Dinâmica dos Fluidos Computacional", *Doctoral thesis*, ITA, CTA, São José dos Campos, SP, Brazil, 258 p.
- Mavriplis, D. J., 1988, "Multigrid Solution of the Two-Dimensional Euler Equations on Unstructured Triangular Meshes", *AIAA Journal*, Vol. 26, No. 7, pp. 824-831.
- Mavriplis, D. J., 1990, "Accurate Multigrid Solution of the Euler Equations on Unstructured and Adaptive Meshes", *AIAA Journal*, Vol. 28, No. 2, pp. 213-221.
- Mavriplis, D. J., 1995, "Multigrid Techniques for Unstructured Meshes", *ICASE Report* No. 95-27.
- Nicola, C., Tognaccini, R., Visingardi, P. and Paparone, L., 1994, "Progress in the Aerodynamic Analysis of Inviscid Supersonic Flow Fields around Complex Aircraft Configurations", *AIAA Paper* 94-1821-CP.
- Radespiel, R., 1989, "A Cell-Vertex Multigrid Method for the Navier-Stokes Equations", *NASA TM*-101557.
- Radespiel, R. and Swanson, R. C., 1995, "Progress with Multigrid Schemes for Hypersonic Flow Problems", *Journal of Computational Physics*, Vol. 116, pp. 103-122.
- Stiles, R. J. and Hoffman, J. D., 1985, "Analysis of Steady, Two-Dimensional, Chemically Reacting, Nonequilibrium, Inviscid Flow in Nozzles", *AIAA Journal*, Vol. 23, No. 3, pp. 342-348.
- Swanson, R. C. and Radespiel, R., 1991, "Cell Centered and Cell Vertex Multigrid Schemes for the Navier-Stokes Equations", *AIAA Journal*, Vol. 29, No. 5, pp. 697-703.

10. Responsibility notice

The author is the only responsible for the printed material included in this paper.